

# Multi-Objective Controller Optimization and Robustness Analysis by the Example of Electro-Mechanical Flight Surface Actuation

*Kolja Michel\*<sup>†</sup> and Christian Schallert\**

*\*Institute of System Dynamics and Control, German Aerospace Center (DLR)  
Muenchner Strasse 20, 82234 Wessling, Germany  
kolja.michel@dlr.de · christian.schallert@dlr.de*

<sup>†</sup>Corresponding author

## Abstract

In this paper the adaption of the software environment 'Multi-Objective Parameter Synthesis' (MOPS) for controller gain optimization is presented. The definition of the optimization criteria, as well as their implementation to the optimization environment are shown. Worst-case searches are conducted to evaluate the effect of uncertainties on the control loop's performance and stability. The methodology of this controller optimization and robustness analysis are demonstrated by means of the torque control for electro-mechanical flight surface actuation. This technology is pursued for future commercial aircraft.

## 1. Introduction

The world is full of optimization problems, and engineers of different disciplines are regularly faced with the challenge of solving them for the technical application. In case of optimization of controller gains, the evaluation of the performance and stability of the control loop is necessary. There is rarely a reference control available against which the results can be compared. Likewise, it is not easy to evaluate whether the optimization result is a local or global minimum. Therefore, the application in practice also requires a check whether the control meets the previously set requirements. This also includes checking whether the behavior is still satisfactory with regard to disturbances, model uncertainties and measurement inaccuracies.

This paper describes the adaptation of a software environment for Multi-Objective Parameter Synthesis<sup>1</sup> for the purpose of controller optimization. To this end, suitable criteria for the evaluation of the control loop with respect to accuracy, oscillation behavior and stability margin are defined. A visual evaluation of the criteria in parallel coordinates is conducted, in which the conflicts of competing criteria become clear. In order to check the robustness of the optimized control loop, worst-case analyses are performed for which measured parameters and plant parameters are subjected to uncertainties in a defined range. The search algorithm is then used to find the respective worst-case constellation of the uncertainties that maximizes a single criterion, e.g. that causes the maximum degradation of the control loops performance. By carrying out this analysis for all criteria defined, it results in several worst-case constellations of the uncertainties. If the criteria still meet the predefined requirements, this confirms the robustness of the control with regard to uncertainties.

Research work is conducted at the Institute of System Dynamics and Control of the German Aerospace Center (DLR) on the design and optimization of a torque control for electro-mechanical flight surface actuation.<sup>2</sup> The described optimization methods are illustrated by means of this application example.

### 1.1 Environment for Multi-Objective Parameter Synthesis (MOPS)

The design of controllers for dynamic systems is a challenging task due to the number of requirements that must be considered and which are mostly in conflict with each other. These requirements include stability, performance and robustness, among others. Therefore, there is a need for a software environment that can aid in the optimization-based design of control systems. One such environment is the Multi-Objective Parameter Synthesis (MOPS), which is primarily based on the technical computing language MATLAB. MOPS facilitates the optimization of system parameters using various optimization algorithms to meet the different requirements of the system. These requirements are then expressed numerically as evaluation criteria for the optimization.<sup>1</sup>

## MULTI-OBJECTIVE CONTROLLER OPTIMIZATION AND ROBUSTNESS ANALYSIS

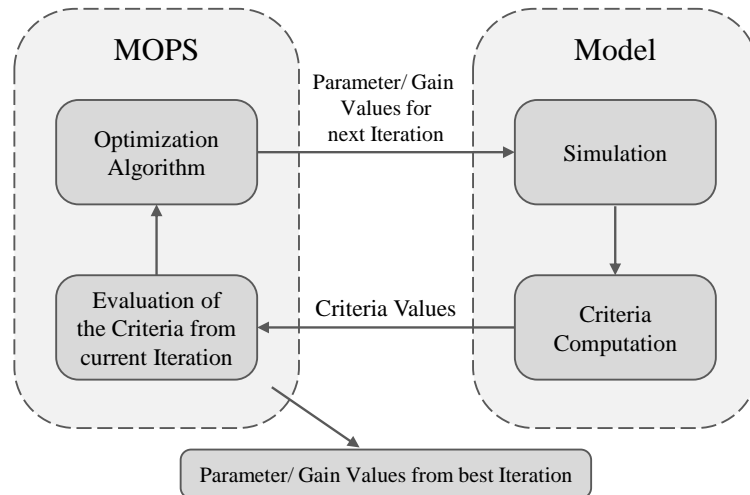


Figure 1: Flow chart of optimization process run through in MOPS

The optimization process in MOPS is illustrated in Figure 1. The separation of the MOPS environment and the simulated model is well visible. In a parameter optimization at first initial parameters are chosen to begin the optimization process. Then, the simulation is performed with mentioned parameters and following this, the evaluation criteria are computed. MOPS reads these in order to assess the most recent iteration. Based on this, the optimization algorithm calculates the controller gains (tuners cf. Figure 2) for the following iteration. The optimization algorithms used for this work will be described in subchapter 3.2. Then, the following simulation is launched. This iterative loop is performed until the defined requirements are satisfied or a predetermined number of iterations have been completed. After each iteration, the actual criteria values are visualized in parallel coordinates. The final output of the optimization process is the parameters from the best iteration.

This describes the process for one case in the optimization. The software environment MOPS allows the definition of multiple cases (see Figure 2) to define for example several operation modes of the simulation model or different environment conditions in which the optimized parameters should be valid. The use case of this will become more clear with the application example in chapter 2.

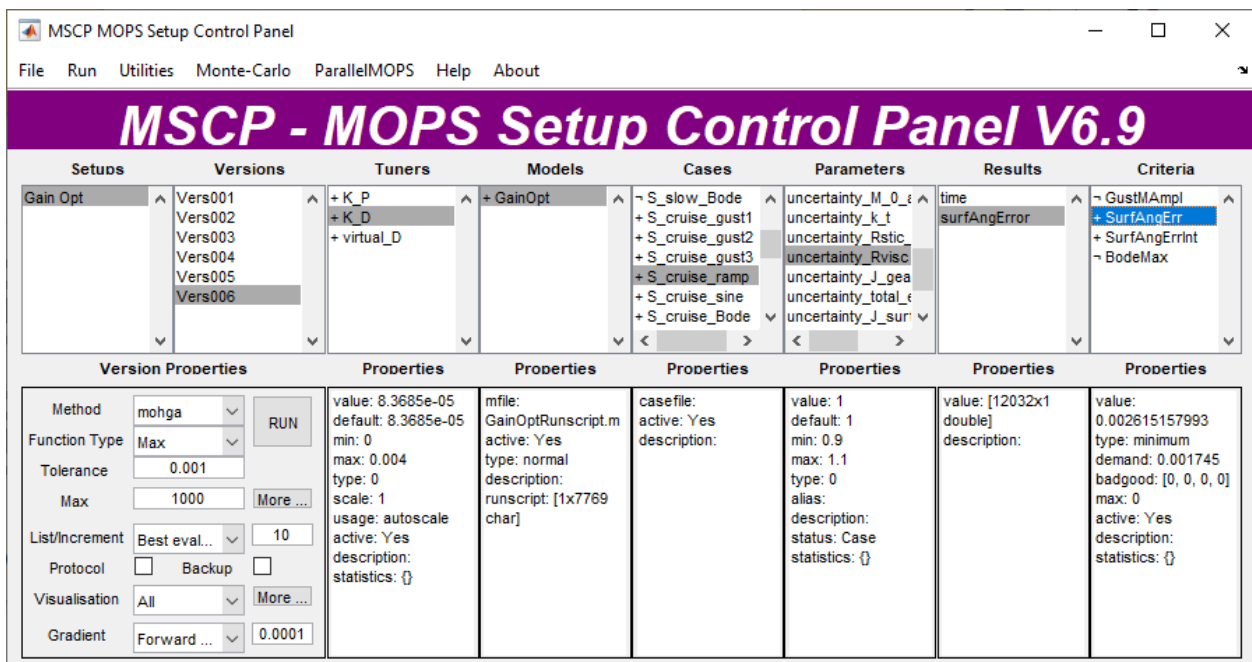


Figure 2: Graphical user interface (GUI) of MOPS

The implementation of the criteria and cases is done through scripts. The user can also employ the graphical user interface (GUI) as shown in Figure 2 to apply some of the functionalities of MOPS. The GUI provides an interactive way to define/adapt the optimization problem and to visualize the results.

## 1.2 Concept of Torque Control for Electro-Mechanical Actuation

For new aircraft research is ongoing to use electro-mechanical actuators (EMA) for primary control surfaces.<sup>3</sup> Hence an adaption of the control to the different actuation technology is meaningful, especially as the dynamics of an EMA is different to hydraulic actuators. In an EMA the motor current is approximately proportional to the actuator output torque. Therefore research work is conducted at the Institute of System Dynamic and Control of the German Aerospace Center (DLR) on the design and optimization of a torque control for electric flight surface actuation.<sup>2</sup> The torque control leads to further advantages over conventional position control as a gust load alleviation functionality, no force fight between two active actuators and a simplification of the flight control.<sup>4</sup> In Figure 3 a scheme of the torque control is shown.

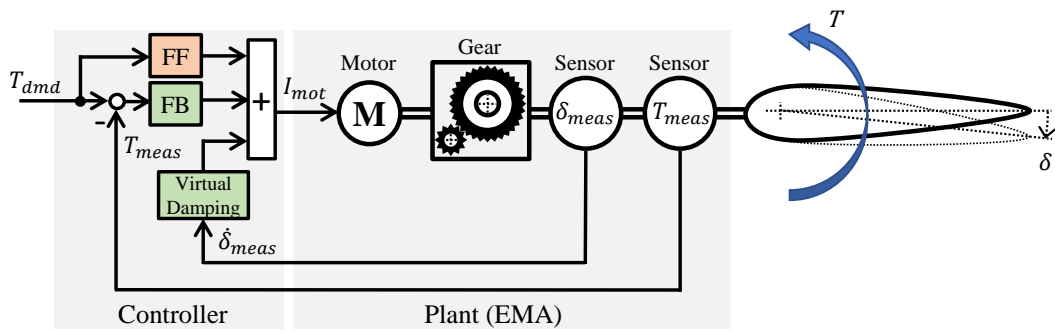


Figure 3: Scheme of the torque control for electro-mechanical actuation

On the right side of Figure 3, there is the actuated control surface with its deflection angle  $\delta$ . The electro-mechanical actuator is illustrated by the motor and the gear, and the two measured magnitudes are the deflection angle and the torque,  $\delta_{meas}$  and  $T_{meas}$  respectively. The torque control is visualized on the left side with its main input  $T_{dmd}$  coming from the flight control computer (FCC). The control consists of a feedforward and feedback, wherein the demanded torque is processed.

The feedforward is an inverse model of the plant, where a demanded motor torque is calculated that considers the demanded torque, the gear ratio, the inertia, the friction and the efficiency of the EMA. Therefore the aerodynamic stiffness  $k_\delta$  is used to calculate the expected movement of the surface based on the demanded torque. The aerodynamic stiffness  $k_\delta$  is the product of the aerodynamic surface torque coefficient  $c_{h\delta}$ , the dynamic pressure  $q$ , the reference surface  $S$  and the reference length  $c$ , and correlates the surface torque  $T$  with the surface angle  $\delta$  as follows:

$$T = c_{h\delta} \cdot q \cdot S \cdot c \cdot \delta = k_\delta \cdot \delta \quad (1)$$

If there were no disturbances or model inaccuracies, the feedforward would be sufficient to control the surface torque. But as there are disturbances, as for example wind gusts, and a model never contains all details of the reality, a feedback is needed to close the control loop. It consists of a proportional and a derivative controller with the gains  $K_p$  and  $K_d$ , respectively. There is as well a virtual damping with the gain  $D_{virt}$  installed, which uses the derivative of the measured actuator stroke  $x_{act,meas}$  to dampen its movements in the case of disturbances. A more detailed view of the control concept can be found in <sup>2,5</sup>.

## 2. Optimization Setup

In order to be able to start an optimization, its boundary conditions must first be defined. For this purpose, the integration of the simulation model into the optimization environment MOPS is described in a setup script. The necessary parameters are also defined. Parameters can then be defined as gains and thus be available as degrees of freedom for the optimization algorithm. For the considered torque control these are the controller gains  $K_p$ ,  $K_d$  and  $D_{virt}$ . As well, multiple cases can be defined to adapt the optimization. These optimization cases are described in the following subchapter by means of the application example.

## 2.1 Optimization Case Definition with the Application Example

The torque control of electro-mechanically actuated flight surfaces has to work in the complete flight envelope. Thus, for the optimization the extreme flight points within the envelope have to be considered as seen in Figure 4. In flight point  $FP_{slow}$  at low airspeed the dynamic pressure  $q$  is low, and thus the aerodynamic stiffness  $k_\delta$  is low. This indicates that larger flight surface deflections are needed to reach a certain surface torque. Flight point  $FP_{VD/MD}$  is at the lowest intersection of the design dive speed  $V_D$  and the corresponding Mach number  $M_D$ . Due to the high airspeed the dynamic pressure is the highest, which leads to a high aerodynamic stiffness. This means that small flight surface deflections are sufficient to reach a certain surface torque. This shows the complexity of the optimization problem.

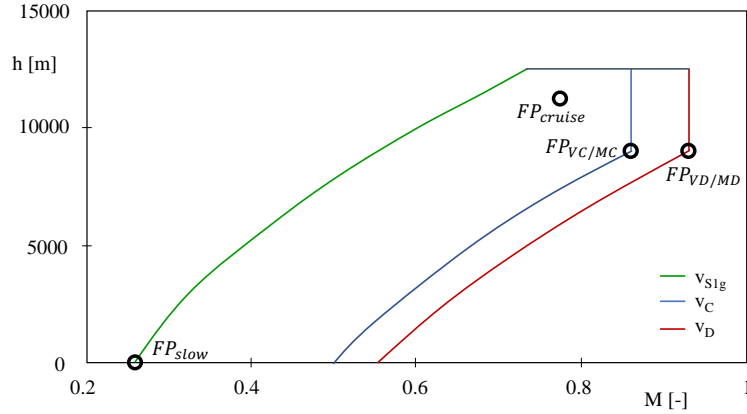


Figure 4: Flight Envelope

For the herein shown optimization procedure the problem is reduced for the sake of brevity to the flight point in cruise flight  $FP_{cruise}$ .

In one flight point a multitude of scenarios can occur and the controller has to be able to respond to all of them. Different input commands for the flight control surface depending on the environmental conditions are possible, as well as disturbances like gusts. This large amount of possible scenarios has to be reduced for the optimization. Thus, all possible scenarios are represented by a ramp-shaped and a sinusoidal torque demand  $T_{dmd}$ , as well as a scenario with constant torque demand but with an incoming gust, which induces a gust torque on the surface  $T_{gust}$ . The gusts are considered with gust gradients  $H$  of 9 m, 58 m and 107 m to cover the full range defined in the CS §25.341 (a).<sup>6</sup> These five operating scenarios are shown in Figure 5.

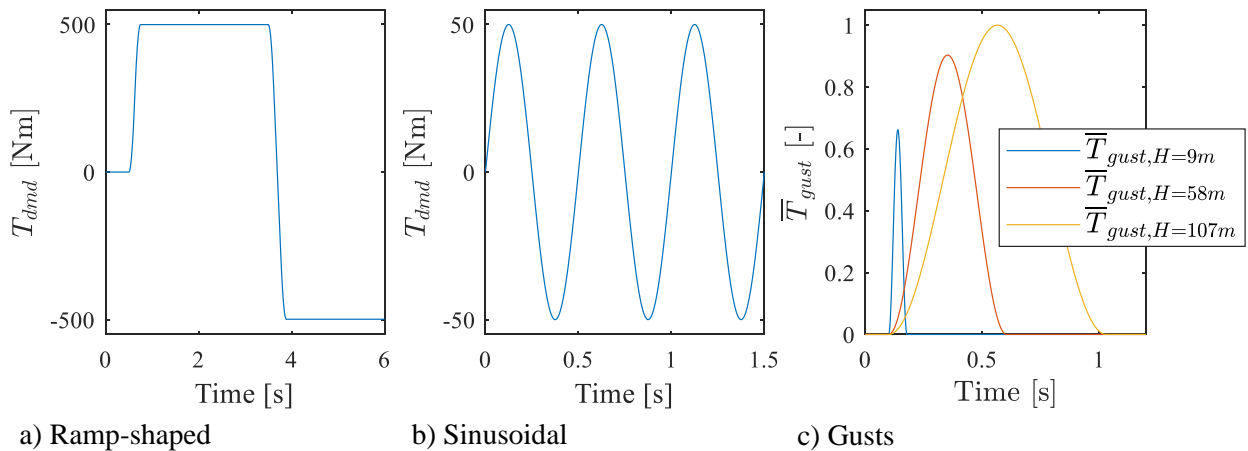


Figure 5: Operating Scenarios

One additional optimization case for each flight point is the evaluation of the frequency response of the linearized model (further explanation in subsection 2.2.3). This leads to six cases for the optimization in flight point  $FP_{cruise}$ .

## 2.2 Evaluation Criteria

For the optimization the evaluation criteria have to be defined according to the requirements. As they have to express numerically the performance and the stability of the control the choice is challenging. It is the goal to achieve the best results possible without violating any concrete requirements. As well some criteria can be more useful in one optimization case than in others. Therefore, in the optimization environment MOPS the evaluation criteria can be activated or deactivated depending on the case. For example for the operating scenarios with the ramp-shaped and sinusoidal torque demand different evaluation criteria are used than in the scenarios with the incoming gusts.

### 2.2.1 Criteria for Scenarios with Specific Torque Demand

The evaluation criteria for scenarios with specific torque demand as a ramp-shaped or a sinusoidal torque demand are defined to grant a good following behavior. For this purpose the control error is regarded. For a torque control the evaluation of the torque error would be obvious, but as requirements are known in general only for conventional position control and to facilitate the comparison, the torque error is converted to a surface angle error  $\delta_{err}$  with the aerodynamical stiffness  $k_\delta$  with equation 1.

To reduce overshoot of the control error the maximal surface angle error  $\delta_{err, max} = \max(|\delta_{err}|)$  is used as an evaluation criterion.

The integral of the surface angle error  $Int_{\delta_{err}}$  is introduced as an additional criterion. Thereby, oscillations or a too slow decline of the angle error leave their imprint on the numerical outcome of this criterion. It is calculated using the following equation:

$$Int_{\delta_{err}} = \int |\delta_{err}| dt \quad (2)$$

### 2.2.2 Criterion for Scenarios with Incoming Gusts

With the torque control comes a gust load alleviation functionality as the flight control surface moves during an incoming gust to keep the torque at the commanded value. This is a very beneficial aspect of the torque control and thus also regarded in the optimization. Here, the maximum torque error  $T_{err, max} = \max(|T_{err}|)$  is used as a criterion. The smaller its value, the more gust load alleviation is achieved.

### 2.2.3 Criterion for Evaluation in the Frequency Domain

For the evaluation of the stability of the control loop a further criterion is needed. Therefore, the dynamic transfer behavior from the demanded torque  $T_{dmd}$  to the resulting torque  $T_{meas}$  of the linearized model is analyzed. One requirement there is, that the amplitude response shall not exceed 2.5 dB, and based on this another criterion is defined as the maximum value of the amplitude response  $Amp_{max}$ . This criterion ensures that the controller gains found during optimization provide sufficient damping and stability margin in the control loop.

### 2.2.4 Weighting of the Criteria

The mentioned criteria  $\delta_{err, max}$ ,  $Int_{\delta_{err}}$ ,  $T_{err, max}$  and  $Amp_{max}$  are all used in the optimization. As they have numerical values of different magnitude, they are divided by reference values that differ depending on the criterion they are used on and the optimization case. By adapting these reference values in between optimization runs the weight on specific criteria can be shifted.

## 3. Implementation of the Optimization

As mentioned the optimization procedure is shown with the application example of a torque control for electro-mechanical flight surface actuation. The flight point during cruise flight  $FP_{cruise}$  is chosen for this demonstration.

### 3.1 Approach

The optimization is performed with the setup defined in section 2 describing the optimization cases and criteria. These are implemented in MOPS via scripts, which also define the GUI (see Figure 2). Then, in between several optimization runs the settings can be changed easily in the GUI. There are various optimization algorithms available and their use is

## MULTI-OBJECTIVE CONTROLLER OPTIMIZATION AND ROBUSTNESS ANALYSIS

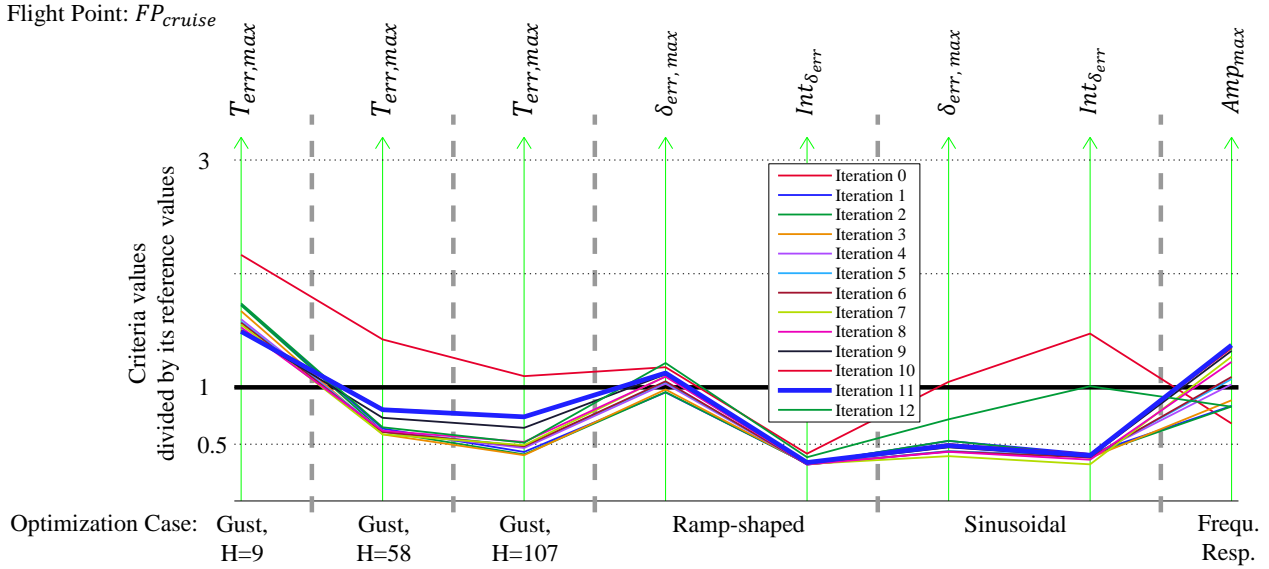


Figure 6: Visualization of optimization run in parallel coordinates

explained in subsection 3.2. After an optimization run the criteria of the iterations are visualized in parallel coordinates as shown in Figure 6. In this visualization the criteria and its respective weighted values are presented on the ordinate. In Figure 6 the conflict between competing criteria can be seen. Typical in this application example is the major conflict between the criterion  $T_{err,max}$  in the scenario with the short gust with  $H=9$  m and the criterion  $Amp_{max}$  from the frequency domain. At some point of the optimization, one criterion is only reducible on the cost of the other. This phenomenon is explained by the conflict in controller design between responsiveness of the control to a short gust resolved by high gains and the stability of the control resolved by lower gains. By adapting the reference values between optimization runs the weight on these criteria can be changed to reach a reasonable trade-off between stability and performance regarding gust load alleviation.

As well, it is necessary to check regularly the simulation results in the time domain, because the criteria, as they are scalar values, can not depict the complete course of the simulation.

### 3.2 Optimization Algorithms

There are several optimization algorithms implemented in the software environment MOPS. The ones used in the herein presented optimization approach are introduced in this section. These are the gradient-based algorithm *sqp*, the genetic algorithm *ga2* and the hybrid approach *mohga*. These different algorithms were used to exploit their individual advantages and thereby avoiding local minima.

The sequential quadratic programming *sqp* (with the MOPS implementation based on <sup>7</sup>) is a gradient-based local optimization method and can be used for general nonlinear programming e.g. solving a nonlinear optimization problem. The version implemented in MOPS considers the bounds on variables and linear constraints and avoids their violation during the iterations. As *sqp* is a gradient-based method the gradients of functions and constraints are needed. Especially when using noisy functions the numerical approximation can cause difficulties. It can lead to a poor gradient approximation and thus slowing down or preventing the convergence of the method. As it is a gradient-based local optimization method, a found solution may not be the global optimum (for example depending on the selected initial parameters). However, *sqp* is very efficient for smooth problems (criteria and constraints), since the descent direction given by the gradient information then allows to achieve a fast super-linear convergence to the respective minimum.

Genetic algorithms are based on evolution principles which lead to the survival of the fittest - most performant - individual. The genetic algorithm *ga2* includes enhanced techniques for selection, crossover and mutation as documented in <sup>8</sup>. For multi-objective optimization the search for Pareto fronts is implemented and crowding distance strategies are applied to keep multiple, highly fit, but significantly different solutions in a generation and thereby avoiding early convergence to local minima.

The multi-objective hybrid genetic algorithm *mohga* is developed by Joos to solve multi-objective optimization problems, i.e. to find approximations of the Pareto front, in MOPS.<sup>9</sup> Therefore *mohga* uses a non-dominated sorting algorithm similar to NSGA-II algorithm.<sup>10</sup> The algorithm is enhanced by recurrent intermediate calls of a local search method like Pattern search or *sqp* to improve the single objective functions separately. Pattern search serves also to further enlarge the solution spread to a better coverage of local or possibly global minima.

### 3.3 Optimization Results

The conducted optimizations results in one set of controller gains for the flight point  $FP_{cruise}$ . The proportional controller gain is  $K_p = 23.5E-3$ , the derivative gain is  $K_d = 18.0E-5$  s and the value for the virtual damping is  $D_{virt} = 57.3$  Ns. Figure 7 shows a simulation of a ramp-shaped torque demand with the above mentioned optimized controller gains for the flight point  $FP_{cruise}$ . In Figure 7 a) the demanded angle  $\delta_{dmd}$  and the measured angle  $\delta_{meas}$  are shown, which are calculated from the according torque with equation 1 due to the reasons explained in section 2.2.1. There is only very little difference between the two courses, and therefore the control error  $\delta_{err} = \delta_{dmd} - \delta_{meas}$  is shown in Figure 7 b). It can be seen, that the stationary angle error remains - despite of the noise - below  $0.03^\circ$ . The control error does not exceed  $0.15^\circ$  in the transient phase. Thus, a high control accuracy is achieved with the optimized controller gains.

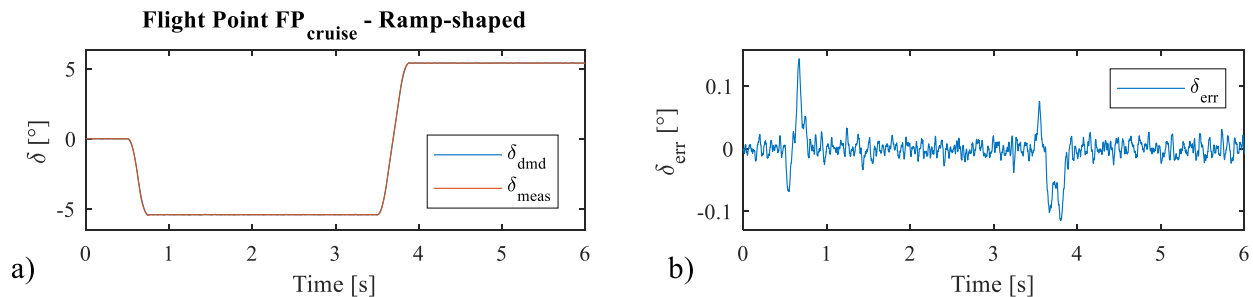


Figure 7: Simulation of ramp-shaped torque demand with optimized controller gains

## 4. Robustness Analysis

Controlled systems can be affected by uncertainties and disturbances that can compromise their performance and stability. The torque control shown here is modeled in a simulation environment and is therefore an approximation of the reality. Hence, a robustness analysis is a critical step in the design and development of the controlled systems, as it evaluates the system's ability to maintain stable and satisfactory performance in the face of uncertainties and disturbances. There are several methods to perform a robustness analysis. Here, worst-case searches are conducted to evaluate the performance of the control in the presence of uncertainties. These are described in the following subchapters, including a description of worst-case search implementation in MOPS, the application to the torque control and its results.

### 4.1 Worst-case Searches with MOPS

A worst-case search aims for the worst case of a criterion. For doing so, the previously optimized controller gains are kept constant and parameters are defined to represent the uncertainty of the plant. Then, in each worst-case search the corresponding criterion is maximized to find the worst combination of the defined uncertainties. So in contrary to the optimization before, the optimized controller gains remain unchanged, and the uncertain parameters are the new degrees of freedom. A worst-case search is performed individually for each criterion of interest and leads to different numeric combinations of uncertain parameters. With these, in the simulation can be seen how much the results can worsen in consideration of the presumed uncertainty ranges. If the results are still acceptable, the robustness regarding uncertainties is shown. Also, it leads to insights how the individual parameters influence the results. In MOPS the worst-case searches are implemented in the GUI. The previous optimization setup is easily convertible to a worst-case setup.

## 4.2 Application of Worst-case Searches

The torque control for flight surface actuation is modeled in a simulation environment. To evaluate its robustness, parameters of the plant are identified which can be subject to uncertainties. These are the stiction coefficient  $R_{stic}$ , the viscous friction coefficient  $R_{visc}$ , the motor torque constant  $k_T$ , the inertia of the gear  $J_{gear}$  and the inertia of the surface  $J_{surf}$ . The uncertainties of these plant parameters can be attributed to production tolerances, aging and changing environmental conditions, such as temperature. As well, the aerodynamic parameters, which are used in the controller, can be subject to uncertainties. These are the control surface related aerodynamic stiffness  $k_\delta$  and the surface torque in the neutral position  $T_{0,aero}$ .

For the worst-case searches an uncertainty range of  $\pm 10\%$  is defined and applied by an uncertainty factor between 0.9 and 1.1 for each of the parameters. These uncertainty factors are then the new degrees of freedom as explained in section 4.1. The worst-case searches are conducted in the considered flight point ( $FP_{cruise}$ ) for each optimization case with the most relevant criterion as the maximized one. This results in six worst-case searches, as shown in Figure 8 and explained in the following section 4.3.

## 4.3 Results

The results of the worst-case searches in flight point  $FP_{cruise}$  are visualized in Figure 8. On the right side the six cases are shown with the considered criterion value after optimization and as the result of the worst-case search. On the left side the found uncertainty factors are shown which lead to the respective worst-case.

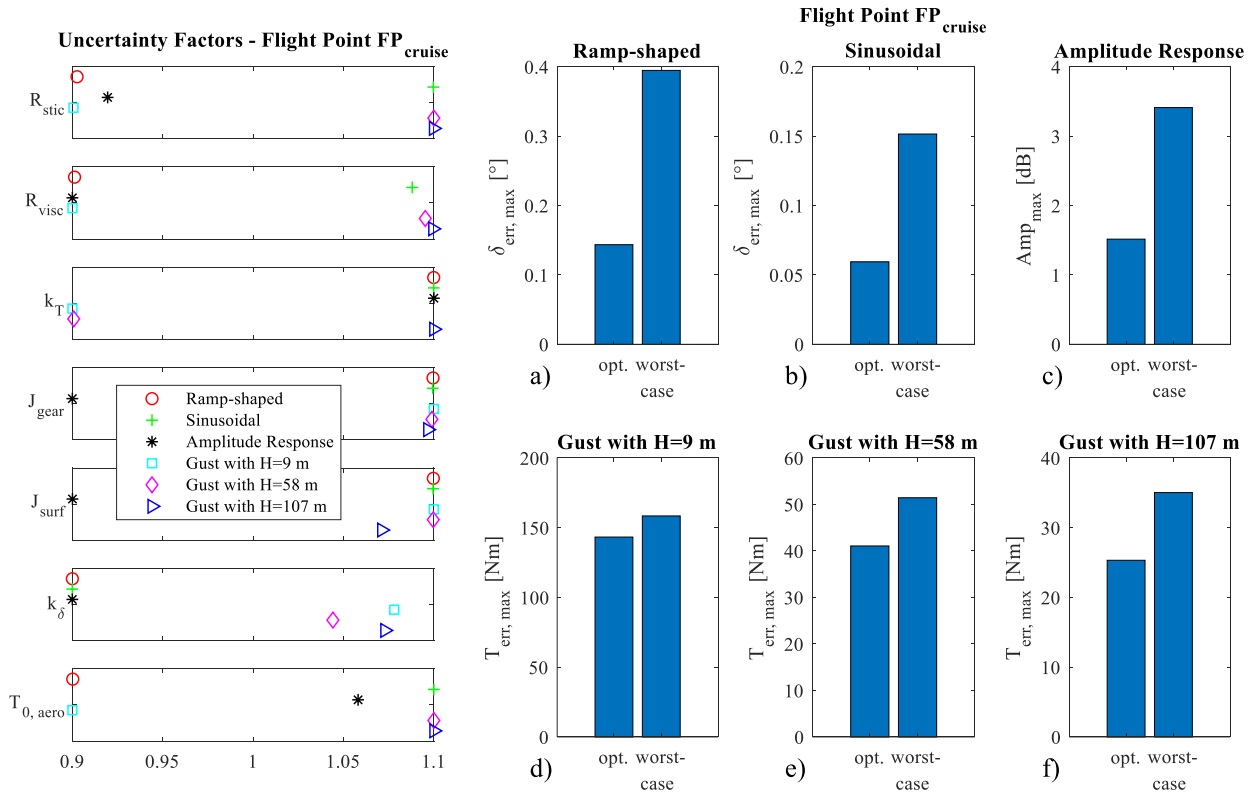


Figure 8: Results of worst-case searches in flight point  $FP_{cruise}$

In Figure 8 a) the results of the worst-case search for a ramp-shaped torque command is shown. The relevant criterion is the maximal angle error  $\delta_{err,max}$ . After optimization the maximal angle error is  $0.14^\circ$  and it is degraded to  $0.39^\circ$  due to the respective worst combination of uncertainty factors. For the sinusoidal torque demand in b) the angle error increases from  $0.06^\circ$  to  $0.15^\circ$ . Since these maximal angle errors occur in the transient phase, their magnitude is tolerable. The stationary angle errors do not exceed  $0.2^\circ$  neither optimized nor in the worst-case.



In Figure 8 c) the behavior of the amplitude response is shown. The value of  $Amp_{max}$  increases from 1.5 dB to 3.4 dB, which means an increase from 1.19 to 1.48 in absolute values. As it is the result of the most unfavorable constellation of uncertainty factors, this is deemed as acceptable.

In Figure 8 d) - f) the results of the operating scenarios with an incoming gust with different gradients are shown. It can be seen that the maximal torque error  $T_{err, max}$  of the respective worst-case is higher and thus the gust load alleviation is reduced. Nevertheless there remains a high gust load alleviation as shown in Figure 9 for the example of a gust with the gradient  $H = 107$  m in flight point  $FP_{cruise}$ . The course of  $T_{gust, tot}$  shows the torque on a rigid, position-controlled flight control surface that does not give way to the disturbance. In comparison, the courses of  $T_{load}$  after optimization and for the worst-case are clearly closer to the demanded torque  $T_{load, dmd}$ , which leads to the mentioned effect of the gust load alleviation. This shows that even with the worst-case constellation of uncertainties a high load alleviation remains in place.

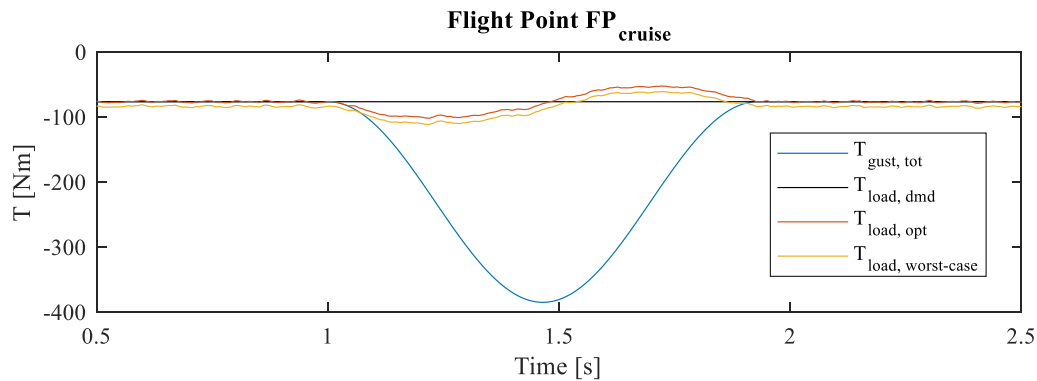


Figure 9: Simulation of a gust penetration with  $H=107$  m

## 5. Summary

Optimization problems are prevalent in various engineering disciplines, and one such challenge is the optimization of controller gains for technical applications.

This paper focuses on adapting a software environment for Multi-Objective Parameter Synthesis (MOPS) for the use of controller gain optimization. Suitable criteria are defined for numerical evaluation of control loop performance with respect to accuracy, oscillation behavior, and stability margin. Computed criteria values are displayed in parallel coordinates, which assists the designer in identifying feasible trade-offs especially between conflicting criteria. The optimization methodology is shown with the application example of a torque controller for electro-mechanical flight surface actuation. Corresponding research work is carried out at the Institute of System Dynamics and Control of the German Aerospace Center (DLR).

In order to assess the robustness of the optimized control loop, (so called) worst-case searches are performed. Performance and stability of the optimized control loop can be (detrimentally) affected by model uncertainty that is expressed by specific ranges of values of the plant and aerodynamic parameters. The search algorithm is then used to find worst-case constellations of uncertain parameters that maximize specific criteria, for instance, causing the maximum degradation of control loop performance. By conducting this analysis for all relevant criteria, several worst-case constellations are obtained. If the control loop still meets the predefined requirements under these conditions, then it confirms the robustness of the optimized control loop when faced with uncertainties.

The proposed optimization methods are demonstrated in one flight point and the results with the optimized controller gains are presented. It shows, that a high control accuracy is achieved. During the worst-case searches the uncertain model parameters are varied in a range of  $\pm 10\%$  and it could be verified that the degradation of performance and stability margin stays limited. Thus, it can be concluded, that the optimization methods led to a robust control.

## 6. Acknowledgments

This research has received funding from the German Federal Ministry for Economic Affairs and Climate Action in the frame of the LuFo VI-1 MODULAR joint research project (FKZ: 20Y1910B) that is conducted from 2020 to 2024.

## References

- [1] H.-D. Joos, J. Bals, G. Looye, K. Schnepfer, and A. Varga, "A multi-objective optimisation-based software environment for control systems design," pp. 7–14, 9 2002.
- [2] C. Schallert and K. Michel, "Torque controller optimization and robustness analysis for electro-mechanical primary flight surface actuation," *AIAA Journal of Guidance, Navigation, and Control (to be published)*, 2023.
- [3] D. Arriola and F. Thielecke, "Model-based design and experimental verification of a monitoring concept for an active-active electromechanical aileron actuation system," *Mechanical Systems and Signal Processing*, vol. 94, pp. 322–345, 9 2017.
- [4] T. S. Pollack, G. H. Looye, and F. L. van der Linden, "Design and flight testing of flight control laws integrating incremental nonlinear dynamic inversion and servo current control," *AIAA Scitech 2019 Forum*, 2019.
- [5] K. Michel and C. Schallert, "Optimisation of a torque controller for electro-mechanical flight surface actuation," *Recent Advances in Aerospace Actuation Systems and Components (to be published)*, 2023.
- [6] Easa, "Certification specifications and acceptable means of compliance for large aeroplanes (CS-25)," 2021.
- [7] K. Schittkowski, "Nonlinear programming codes : Information, tests, performance," p. 242, 1980.
- [8] A. Eiben and J. Smith, *Introduction to Evolutionary Computation*. Springer, 2007.
- [9] H.-D. Joos, "MOPS - Multi-objective parameter synthesis, user's guide V6.6," *DLR Technical Report*, 2016.
- [10] K. Deb, A. Pratap, S. Agarwal, and T. Meyarivan, "A fast and elitist multiobjective genetic algorithm: NSGA-II," *IEEE Transactions on Evolutionary Computation*, vol. 6, pp. 182–197, 4 2002.